

Date of publication xxxx 00, 0000, date of current version xxxx 00, 0000.

Digital Object Identifier 10.1109/ACCESS.2018.DOI

# Quantum Turbo Decoding for Quantum Channels Exhibiting Memory

**MOHD AZRI MOHD IZHAR<sup>1</sup>, ZUNAIRA BABAR<sup>2</sup>, HUNG VIET NGUYEN<sup>3</sup>, PANAGIOTIS BOT SINIS<sup>2</sup>, DIMITRIOS ALANIS<sup>2</sup>, DARYUS CHANDRA<sup>2</sup>, SOON XIN NG<sup>2</sup>, AND LAJOS HANZO<sup>2</sup>**

<sup>1</sup>Wireless Communication Center and Ubiquitous Broadband Access Network (U-BAN) Group, UTM Razak School of Engineering and Advanced Technology, Universiti Teknologi Malaysia, Jalan Sultan Yahya Petra, Kuala Lumpur, 54100, Malaysia (e-mail: mohdazri.kl@utm.my)

<sup>2</sup>School of Electronics and Computer Science, University of Southampton, Southampton, SO17 1BJ, United Kingdom (email: {zb2g10, pb1y14, da4g11, dc2n14, sxn, lh}@ecs.soton.ac.uk)

<sup>3</sup>5G Innovation Centre, University of Surrey, Guildford, GU2 7XH, United Kingdom (email: hung.nguyen@surrey.ac.uk)

Corresponding author: Lajos Hanzo (e-mail: lh@ecs.soton.ac.uk).

This work was supported in part by the Malaysian Ministry of Higher Education, in part by the UTM Razak School of Engineering and Advanced Technology, Universiti Teknologi Malaysia under HIGDR Grant R.K130000.7740.4J314, in part by the European Research Council through the Advanced Fellow Grant, and in part by the Royal Society's Wolfson Research Merit Award.

**ABSTRACT** Inspired by the success of classical turbo codes, quantum turbo codes (QTCs) have also been conceived for near-hashing-bound transmission of quantum information over memoryless quantum channels. However, in real physical situations, the memoryless channel assumption may not be well justified since the channel often exhibits memory of previous error events. Here, we investigate the performance of QTCs over depolarizing channels exhibiting memory and we show that they suffer from a performance degradation at low depolarizing probability values. In order to circumvent the performance degradation issue, we conceive a new coding scheme termed as quantum turbo coding scheme exploiting error-correlation (QTC-EEC) that is capable of utilizing the error-correlation while performing the iterative decoding at the receiver. The proposed QTC-EEC can achieve convergence threshold at a higher depolarizing probability for channels with a higher value of correlation parameter and achieve performance near to the capacity. Finally, we propose a joint decoding and estimation scheme for our QTC-EEC relying on correlation estimation (QTC-EEC-E) designed for more realistic quantum systems with unknown correlation parameter. Simulation results reveal that the proposed QTC-EEC-E can achieve the same performance as that of the ideal system of known correlation parameter and hence, demonstrate the accurate estimation of the proposed QTC-EEC-E.

**INDEX TERMS** Quantum channels with memory, quantum turbo codes, iterative decoding, quantum error-correction codes, Markovian correlated-noise, Markov process.

## I. INTRODUCTION

QUANTUM computing and communication exploit the unique properties of quantum mechanics, such as the superposition of states and entanglement [1] to provide inherently fast and secure data processing. However, the quantum bits (qubits) are intrinsically fragile and susceptible to quantum decoherence imposed by the unavoidable interaction between the qubits and the environment, inflicting qubit errors. Therefore, the practical realization of a quantum system relies on the preservation of the quantum coherence of a quantum state. In order to mitigate the detrimental effects of quantum decoherence, several approaches have been proposed [2]–[5], including the most well-known approach

of quantum error-correction codes (QECCs) [2].

QECCs make use of redundant auxiliary (also called ancilla) qubits to protect the data qubits. The first quantum code was introduced by Shor in 1995 [2] that was only capable of correcting a single qubit error in a nine-qubit block code. Since then, many other QECCs have been developed that can outperform the Shor's nine-qubit code, with the goal of approaching the quantum channel's capacity. Inspired by the near-capacity performance of the classical turbo codes [6], quantum serial turbo codes or also known as quantum turbo codes (QTCs) were conceived in [7], [8] and later extended for entanglement-assisted coding schemes in [9]–[12]. The superiority of QTCs in the context of memoryless

depolarizing channels was demonstrated in [7]–[12], where the QTCs were shown to exhibit a similar turbo-cliff region to their classic counterparts in the vicinity of the quantum channel's capacity. Another near-capacity quantum code family is constituted by low density parity check (QLDPC) codes [13]–[15]. However, it has been shown that there are several decoding issues associated with QLDPC codes. Firstly, the belief propagation decoding algorithm of QLDPC codes is not capable of exploiting the degenerate errors. Furthermore, the unavoidable length-4 cycles found in QLDPC codes degrade their performance [8], [11]. Fortunately, all these weaknesses of QLDPC codes can be circumvented by QTCs can also offer a higher flexibility in terms of choosing the code parameters such as the frame length, coding rate, constraint length and interleaver type.

The designers of QECCs have typically assumed that the channels are memoryless, where the errors inflicted on the transmitted qubits are identically and independently distributed (i.i.d). However, in real physical situations, the memoryless channel assumption may only be valid upon applying an external magnetic field to reset the channel's memory or by transmitting the successive signals at a sufficiently low rate to allow the channels to naturally subside before transmitting the next signal [16], [17]. Despite that, this is not justified in a high-rate communication system where the signals follow each other in quick succession. Physical examples of channels exhibiting a memory in quantum information processing are constituted by unmodulated spin chains [18], [19], micromasers [20], and fibre optics [21], [22].

The quantum channel's memory effect were first studied in 2002 by Macchiavello *et al.* [23] for classical information transmission over a depolarizing channel and it was demonstrated that for a certain correlation value, encoding the classical information into maximally entangled quantum states is capable of enhancing the channel capacity over the product quantum states encoding for two successive channel uses. This work was then extended to quasi-classical depolarizing channels [24], to Pauli channels [25], to more than two successive uses of Pauli channels [26] and to superdense-coded qudit<sup>1</sup> Pauli channels [27]. A model and a unitary representation of quantum channels with memory for classical and quantum information was introduced by Bowen *et al.* in [28]. In 2005, a unified framework for quantum channels exhibiting memory was developed by Kretschmann *et al.* in [17], where the upper bounds of classical and of quantum channel capacities were derived for various scenarios, depending on whether the transmitter, the receiver or the eavesdropper has the control on the initial and final memory states. Most of the theoretical contributions on discrete quantum channels with memory assume contamination by Markovian correlated noise, since the properties of typical sequences generated by a Markov process are well understood [23]–

[35].

Since most of the existing QECCs including QTCs [7]–[12] are designed for memoryless channels, these QECCs may not perform well for channels with memory. There have been several studies on the performance of the existing QECCs in the context of quantum channels exhibiting memory, specifically using the 3-qubit repetition code [31], [32], [35], [36], CSS codes [36] and stabilizer codes [33]. The performance degradation of the existing QECCs became more severe as the error-correlation of the quantum channels became higher. In [35], [36], the authors proposed concatenated coding schemes relying on the 3-qubit repetition code and a specific code based on the decoherence-free subspace formalism of [5] which was investigated in the context of a bit-flip (or a phase-flip) quantum channel. Although the performance of this concatenated code improved upon increasing the error-correlation, but for memoryless channels and channels associated with low error-correlation, the stand alone 3-qubit code outperformed the concatenated code. For a recent review on quantum channels with memory please refer to [16].

Against this background, we design a new QTC-based coding scheme for depolarizing channels exhibiting memory. The correlated errors are modeled by a 4-state Markov chain and the error-correlation characterized by the transition probabilities are exploited using our modified maximum *a posteriori* (MAP) algorithm employed by the inner decoder. In contrast to the concatenated coding schemes of [35], [36] that are only suitable for a certain range of error-correlations, our proposed coding scheme is capable of achieving performance gains over the existing QTCs for the entire range of error-correlations and does not suffer from any performance degradation for transmission over memoryless channels. Hence, our novel contributions can be summarized as follows:

- 1) *We conceive a quantum turbo coding scheme exploiting the error-correlation (QTC-EEC), when performing syndrome-based iterative decoding. This is realized by modifying the MAP algorithm employed by the inner decoder to capitalize on the statistics of the error-correlation. The proposed QTC-EEC outperforms the existing QTCs and achieves higher performance gains over the existing QTCs, when the error-correlation is increased. Moreover, we demonstrate the accuracy of extrinsic information transfer (EXIT) charts of QTC-EEC, which is important for EXIT-chart based code design/optimization.*
- 2) *We propose a joint decoding and estimation technique for our QTC-EEC relying on correlation estimation (QTC-EEC-E). We demonstrate that the proposed QTC-EEC-E is capable of accurately estimating the unknown correlation parameter  $\mu$  and achieves the same performance as that when  $\mu$  is perfectly known at the receiver.*

It is worth mentioning that although we specifically consider unassisted transmission over a depolarizing channel in

<sup>1</sup>Qudit is the generalization of a qubit for a  $d$ -level quantum state where a qubit corresponds to a 2-level quantum state.

this paper, the proposed QTC-EEC and QTC-EEC-E can also be applied for entanglement-assisted transmissions [10] as well as for communicating over any Pauli channels, even in conjunction with asymmetric error probabilities [37]. The remainder of this paper is organized as follows. Our system model and the channel capacity of quantum channels associated with Markovian correlated noise are described in Section II. Section III investigates the performance of the existing QTCs for transmission over a quantum channel with memory. The proposed QTC-EEC is detailed in Section IV. Joint decoding and estimation of the correlation parameter is proposed and analyzed in Section V. Finally, concluding remarks are provided in Section VI.

## II. QUANTUM CHANNELS EXHIBITING MEMORY

In many contributions related to quantum channels exhibiting memory, a class of quantum channels subjected to discrete Markovian correlated noise was considered [23]–[35]. Similarly, in this paper we also consider the same class of channels characterizing the temporal correlation between the errors introduced by the quantum channels. The error model presented in this section is based on the general Pauli channels, which include the family of depolarizing channels.

### A. MODEL OF QUANTUM CHANNELS EXHIBITING MEMORY

For a memoryless Pauli channel, the completely positive trace-preserving mapping of an input quantum state having a density operator  $\rho$  in its operator-sum (or Kraus) representation [38] is given by [39]:

$$\begin{aligned}\Phi(\rho) &= \sum_{\mathcal{A} \in \{\mathbf{I}, \mathbf{X}, \mathbf{Y}, \mathbf{Z}\}} p_{\mathcal{A}} \mathcal{A} \rho \mathcal{A} \\ &= p_{\mathbf{I}} \mathbf{I} \rho \mathbf{I} + p_{\mathbf{X}} \mathbf{X} \rho \mathbf{X} + p_{\mathbf{Y}} \mathbf{Y} \rho \mathbf{Y} + p_{\mathbf{Z}} \mathbf{Z} \rho \mathbf{Z},\end{aligned}\quad (1)$$

where  $\mathbf{I}$ ,  $\mathbf{X}$ ,  $\mathbf{Y}$ , and  $\mathbf{Z}$  are Pauli operators defined by [39]:

$$\begin{aligned}\mathbf{I} &= \begin{pmatrix} 1 & 0 \\ 0 & 1 \end{pmatrix}, \quad \mathbf{X} = \begin{pmatrix} 0 & 1 \\ 1 & 0 \end{pmatrix}, \\ \mathbf{Y} &= \begin{pmatrix} 0 & -i \\ i & 0 \end{pmatrix}, \quad \mathbf{Z} = \begin{pmatrix} 1 & 0 \\ 0 & -1 \end{pmatrix},\end{aligned}\quad (2)$$

and  $\{p_{\mathbf{I}}, p_{\mathbf{X}}, p_{\mathbf{Y}}, p_{\mathbf{Z}}\}$  are the probabilities of the Pauli operators  $\{\mathbf{I}, \mathbf{X}, \mathbf{Y}, \mathbf{Z}\}$  that are imposed on the input density operator  $\rho$ , respectively. Naturally, the sum of all the probabilities, i.e.  $p_{\mathbf{I}} + p_{\mathbf{X}} + p_{\mathbf{Y}} + p_{\mathbf{Z}}$  is equal to 1. For depolarizing channels, we have  $p_{\mathbf{X}} = p_{\mathbf{Y}} = p_{\mathbf{Z}} = p/3$  and  $p_{\mathbf{I}} = 1 - p$ , where  $p$  is the depolarizing probability. Here, we define the set of  $\{\mathbf{I}, \mathbf{X}, \mathbf{Y}, \mathbf{Z}\}$  Pauli operators as the effective Pauli group  $\mathcal{G}_1$  applied to a single qubit, while the general effective Pauli group  $\mathcal{G}_N$  applied to  $N$  qubits is an  $N$ -fold tensor product of  $\mathcal{G}_1$  [8], [11].

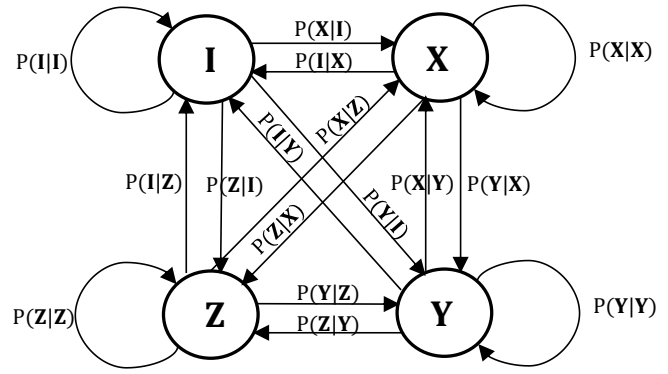


FIGURE 1: The state diagram of a Markov chain where  $\{\mathbf{I}, \mathbf{X}, \mathbf{Y}, \mathbf{Z}\}$ -state correspond to the  $\{\mathbf{I}, \mathbf{X}, \mathbf{Y}, \mathbf{Z}\}$  Pauli operators, respectively.

Let us now consider  $N$  successive uses of the memoryless channel described by Eq. (1) yielding

$$\begin{aligned}\Phi^N \left( \rho^{(N)} \right) &= \sum_{\mathcal{A}_1 \mathcal{A}_2 \dots \mathcal{A}_N \in \mathcal{G}_N} p_{\mathcal{A}_1 \mathcal{A}_2 \dots \mathcal{A}_N} \\ &\cdot (\mathcal{A}_1 \otimes \mathcal{A}_2 \otimes \dots \otimes \mathcal{A}_N) \rho^{(N)} (\mathcal{A}_1 \otimes \mathcal{A}_2 \otimes \dots \otimes \mathcal{A}_N),\end{aligned}\quad (3)$$

where  $\mathcal{A}_i \in \mathcal{G}_1$  is the Pauli operator acted on the  $i$ -th use of the channel with  $i \in \{1, 2, \dots, N\}$ . The joint probability obeys  $p_{\mathcal{A}_1 \mathcal{A}_2 \dots \mathcal{A}_N} = p_{\mathcal{A}_1} \cdot p_{\mathcal{A}_2} \cdot \dots \cdot p_{\mathcal{A}_N}$ , since the errors are imposed independently on each successive channel use. In this case, Eq. (3) can be expressed as an  $N$ -fold tensor product of Eq. (1) to yield  $\Phi^N \left( \rho^{(N)} \right) = [\Phi(\rho)]^{\otimes N}$ .

For channels with memory, the correlation of the errors on each successive channel use can be described by the 4-state Markov chain illustrated in Fig. 1, where the 4 states correspond to the  $\mathbf{I}$ ,  $\mathbf{X}$ ,  $\mathbf{Y}$  and  $\mathbf{Z}$  Pauli operators imposed on the transmitted qubits. The probability of traversing from a previous state  $\mathcal{A}'$  to the current state  $\mathcal{A}$  is denoted as  $q_{\mathcal{A}'|\mathcal{A}}$ , which is equal to the conditional probability of  $P(\mathcal{A}|\mathcal{A}')$ , where  $\{\mathcal{A}', \mathcal{A}\} \in \mathcal{G}_1$ . The error-correlation can be characterized by the correlation parameter  $\mu$  where  $\mu \in [0, 1]$ , with  $\mu = 0$  indicating zero correlation (memoryless channels) and  $\mu = 1$  indicating perfect correlation. In reality,  $\mu$  can be quantified from the time delay  $\Delta t$  between two successive channel uses and the typical relaxation time constant  $\tau$  of the channel environment, which can be expressed as  $\mu \simeq \exp(-\Delta t/\tau)$  [40], [41]. The relationship between the transition probability  $q_{\mathcal{A}'|\mathcal{A}}$  and the correlation parameter  $\mu$  is given by

$$q_{\mathcal{A}'|\mathcal{A}} = (1 - \mu) \cdot p_{\mathcal{A}} + \mu \cdot \delta_{\mathcal{A}'|\mathcal{A}}, \quad (4)$$

where  $\delta_{\mathcal{A}'|\mathcal{A}}$  is the Kronecker delta function and  $p_{\mathcal{A}}$  is the probability of the Pauli operator  $\mathcal{A}$  being imposed on the transmitted qubits. The joint probability in Eq. (3) can be computed as  $p_{\mathcal{A}_1 \mathcal{A}_2 \dots \mathcal{A}_N} = p_{\mathcal{A}_1} \cdot q_{\mathcal{A}_2|\mathcal{A}_1} \cdot \dots \cdot q_{\mathcal{A}_N|\mathcal{A}_{N-1}}$  and

therefore, the completely positive trace-preserving mapping for channels with memory can be represented as [23], [28]

$$\Phi^N \left( \rho^{(N)} \right) = \sum_{\mathcal{A}_1, \mathcal{A}_2, \dots, \mathcal{A}_N \in \mathcal{G}_N} p_{\mathcal{A}_1} \cdot q_{\mathcal{A}_2 | \mathcal{A}_1} \cdot \dots \cdot q_{\mathcal{A}_N | \mathcal{A}_{N-1}} \cdot (\mathcal{A}_1 \otimes \mathcal{A}_2 \otimes \dots \otimes \mathcal{A}_N) \rho^{(N)} (\mathcal{A}_1 \otimes \mathcal{A}_2 \otimes \dots \otimes \mathcal{A}_N). \quad (5)$$

### B. CHANNEL CAPACITY OF DEPOLARIZING CHANNELS EXHIBITING MEMORY

The maximum amount of information that can be reliably sent over the quantum channel at an arbitrarily low probability of error is given by the channel capacity [42]. In general, there are two types of capacities for quantum channels, namely the classical and the quantum channel capacities that correspond to the transmission of classical and of quantum information through the quantum channels, respectively. In this treatise, we particularly consider the transmission of quantum information over the quantum channels with memory. However, at the time of writing, the exact quantum capacity for the transmission of quantum information over the quantum channels with memory has only been found for a few specific channel models, as exemplified by the dephasing channels [30], the amplitude-damping channels [43], and the bit/phase-flip channels [34]. The exact quantum capacity of the general Pauli channels including the depolarizing channels has not been found, hence we will use the lower capacity bound derived in [34].

The lower bound of the quantum capacity derived for the depolarizing channel with memory and having the correlation coefficient  $\mu$  as well as the depolarizing probability  $p$  is given by [34]

$$C_Q^M(\mu, p) = \lim_{N \rightarrow \infty} \frac{1}{N} \left[ I_c^{(1)}(p) + (N-1) \cdot I_c^{(2)}(\mu, p) \right], \quad (6)$$

where  $I_c^{(1)}(p)$  and  $I_c^{(2)}(\mu, p)$  represent the coherent information associated with the first and subsequent transmissions after the first, respectively. These coherent information contributions can be computed using the equations below [34]:

$$I_c^{(1)}(p) = 1 - H_b(p) - p \cdot \log_2(3), \quad (7)$$

$$I_c^{(2)}(\mu, p) = 1 + r_0 \cdot (1-p) \cdot \log_2(r_0) + r_1 \cdot p \cdot \log_2(r_1) + r_2 \cdot (3-p) \cdot \log_2(r_2) + r_3 \cdot p \cdot \log_2(r_3), \quad (8)$$

where we have the binary entropy function  $H_b(p) = -p \cdot \log_2(p) - (1-p) \cdot \log_2(1-p)$ ,  $r_0 = (1-p) \cdot (1-\mu) + \mu$ ,  $r_1 = (1-p) \cdot (1-\mu)$ ,  $r_2 = \frac{p}{3} \cdot (1-\mu)$ , and  $r_3 = \frac{p}{3} \cdot (1-\mu) + \mu$ . In the case of a memoryless channel, substituting  $\mu = 0$  into Eq. (8) will yield  $I_c^{(2)}(0, p) = 1 - H_b(p) - p \cdot \log_2(3)$ . Hence, the corresponding quantum capacity of Eq. (6) becomes  $C_Q^M(0, p) = 1 - H_b(p) - p \cdot \log_2(3)$  for any value of  $N$ . The resultant  $C_Q^M(0, p)$  value is the same as the hashing bound of  $C_Q(p) = 1 - H_b(p) - p \cdot \log_2(3)$ , which sets the lower bound of communicating over a memoryless depolarizing channel [44].

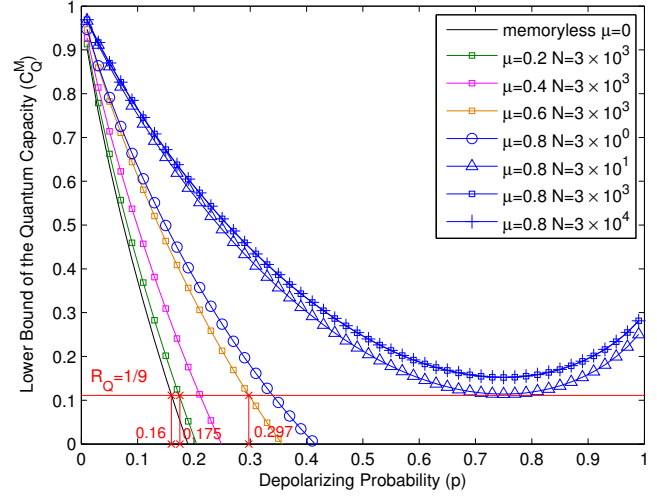


FIGURE 2: Quantum capacity for depolarizing channels exhibiting memory associated with various  $\mu$  and  $N$  values.

Fig. 2 depicts the effect of both the correlation coefficient  $\mu$  and of the number of channel uses  $N$  on the lower bound of the quantum capacity of the depolarizing channel subjected to the Markovian correlated noise of Eq. (6). An increased capacity is observed for a channel having a higher value of  $\mu$ . Furthermore, when relying on more channel uses for transmitting more qubits over the quantum channels would also increase the attainable capacity, as shown for the channel having  $\mu = 0.8$  in Fig. 2, when the value of  $N$  increases from  $3$  to  $3 \times 10^4$ . However, the difference in capacity becomes insignificant for large values of  $N$  such as, for example  $N = 3 \times 10^3$  to  $N = 3 \times 10^4$ . For a desired quantum coding rate, the increase in capacity can also be viewed as an increase in the noise limit  $p^*$ , where reliable quantum communications can be guaranteed. For example, a quantum system with a coding rate of  $R_Q = 1/9$ , the noise limit improves from  $p^* = 0.175$  for the quantum channel having  $\mu = 0.2$  to  $p^* = 0.297$  for that associated with  $\mu = 0.6$ , which tells us that a quantum system communicating over a more correlated channel has a higher noise-tolerance.

### III. EXISTING QTCS TRANSMITTED OVER A QUANTUM CHANNEL EXHIBITING MEMORY

In this section, we will first give an overview of the existing QTCS [8], [11] and then evaluate the performance of the existing QTCS for transmission over depolarizing channels with memory using Monte Carlo simulations.

#### A. EXISTING QUANTUM TURBO CODES

Fig. 3 illustrates the block diagram of a QTC relying on the serial concatenation of two stabilizer codes. An  $[n, k]$  quantum code maps  $k$  logical qubits (uncoded qubits) onto  $n$  physical qubits (encoded qubits) using  $(n-k)$  auxiliary qubits  $|0_{n-k}\rangle$ , where  $n > k$ . For an  $[n, k]$  quantum convolutional code (QCC) with  $m$  memory qubits, the parameter set can be presented as  $[n, k, m]$ . In this work, we employ an

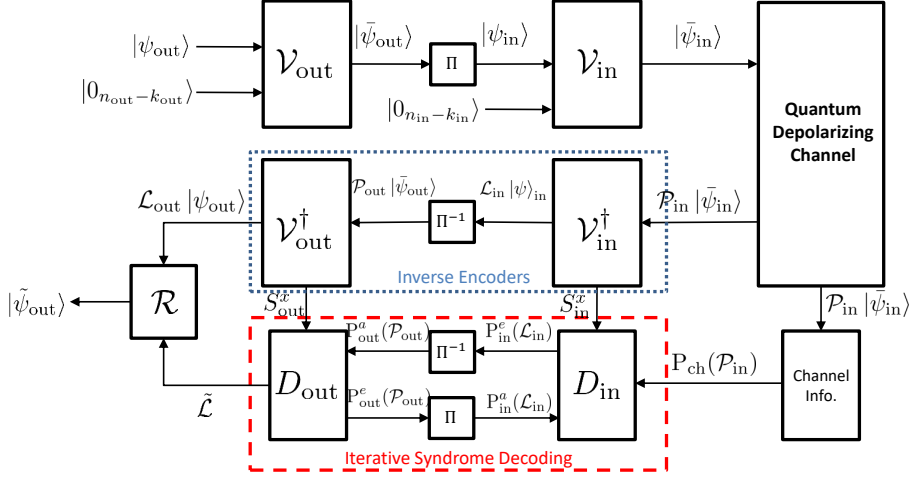


FIGURE 3: System model of a quantum communication system relying on a QTC transmitted over a depolarizing channel exhibiting memory.

$[n_{\text{out}}, k_{\text{out}}, m_{\text{out}}]$  QCC as the outer code and an  $[n_{\text{in}}, k_{\text{in}}, m_{\text{in}}]$  QCC as the inner code. At the transmitter, the logical qubits  $|\psi_{\text{out}}\rangle$  are first encoded to physical qubits  $|\bar{\psi}_{\text{out}}\rangle$  using the outer encoder  $\mathcal{V}_{\text{out}}$  before being interleaved by the quantum interleaver  $\Pi$ . The interleaved qubits  $|\bar{\psi}_{\text{in}}\rangle$  which correspond to the logical qubits for the inner encoder  $\mathcal{V}_{\text{in}}$  are then encoded to  $n = n_{\text{out}} \times n_{\text{in}}$  physical qubits  $|\bar{\psi}_{\text{in}}\rangle$ . The physical qubits  $|\bar{\psi}_{\text{in}}\rangle$  are serially transmitted over a depolarizing channel having a depolarizing probability  $p$ . The channel inflicts an  $n$ -tuple error  $\mathcal{P}_{\text{in}} \in \mathcal{G}_n$  on the transmitted qubits  $|\bar{\psi}_{\text{in}}\rangle$ .

At the receiver, the corrupted physical qubits  $\mathcal{P}_{\text{in}} |\bar{\psi}_{\text{in}}\rangle$  are passed to the inverse encoder  $\mathcal{V}_{\text{in}}^{\dagger}$  to yield the corrupted logical qubits of the inner encoder  $\mathcal{L}_{\text{in}} |\psi_{\text{in}}\rangle$  and the  $(n_{\text{in}} - k_{\text{in}})$  syndrome qubits  $\mathcal{S}_{\text{in}} |0_{n_{\text{in}}-k_{\text{in}}}\rangle$ . The syndrome sequence  $|0_{n_{\text{in}}-k_{\text{in}}}\rangle$  is invariant to the Z-component of  $\mathcal{S}_{\text{in}}$  and therefore, the syndrome qubits  $\mathcal{S}_{\text{in}} |0_{n_{\text{in}}-k_{\text{in}}}\rangle$  collapse to the X-component of the classical syndrome bits  $S_{\text{in}}^x$  upon measurement [8], [11]. The erroneous logical qubits  $\mathcal{L}_{\text{in}} |\psi_{\text{in}}\rangle$  are deinterleaved by  $\Pi^{-1}$  to result in the erroneous physical qubits of the outer inverse encoder  $\mathcal{V}_{\text{out}}^{\dagger}$ , which are then processed by  $\mathcal{V}_{\text{out}}^{\dagger}$ . This results in the potentially erroneous decoded logical qubits of the outer encoder  $\mathcal{L}_{\text{out}} |\psi_{\text{out}}\rangle$  and the  $(n_{\text{out}} - k_{\text{out}})$  syndrome qubits  $\mathcal{S}_{\text{out}} |0_{n_{\text{out}}-k_{\text{out}}}\rangle$  that collapse to the classical syndrome bits  $S_{\text{out}}^x$  upon measurement.

A degenerate iterative decoding scheme [8] is invoked for the pair of classic syndrome-based SISO decoders, namely the inner SISO decoder  $D_{\text{in}}$  and the outer SISO decoder  $D_{\text{out}}$  for estimating the error coset  $\tilde{\mathcal{L}}_{\text{out}}$  inflicted on the logical qubits of the outer encoder. The channel information  $P_{\text{ch}}(\mathcal{P}_{\text{in}})$ , the classic syndrome bits  $S_{\text{in}}^x$  and the *a priori* information  $P_{\text{in}}^a(\mathcal{L}_{\text{in}})$  (equiprobable for the first iteration) are processed by  $D_{\text{in}}$  to compute the extrinsic information  $P_{\text{in}}^e(\mathcal{L}_{\text{in}})$ , which is related to the error inflicted on the logical qubits of the inner encoder. The extrinsic information  $P_{\text{in}}^e(\mathcal{L}_{\text{in}})$  is then de-interleaved by  $\Pi^{-1}$  and fed to  $D_{\text{out}}$  as

the *a priori* information  $P_{\text{out}}^a(\mathcal{L}_{\text{out}})$ . The computation of the *a posteriori* information  $P_{\text{out}}^o(\mathcal{L}_{\text{out}})$  and the extrinsic information  $P_{\text{out}}^e(\mathcal{P}_{\text{out}})$  is performed by  $D_{\text{out}}$  using the *a priori* information  $P_{\text{out}}^a(\mathcal{L}_{\text{out}})$ , and the classic syndrome bits  $S_{\text{out}}^x$ . The extrinsic output  $P_{\text{out}}^e(\mathcal{P}_{\text{out}})$  is then interleaved by  $\Pi$  to yield  $P_{\text{in}}^a(\mathcal{L}_{\text{in}})$ , which is fed back to  $D_{\text{in}}$  for the next iteration. This process is repeated until convergence is achieved or the preset number of iterations is reached. Finally, based on the *a posteriori* information  $P_{\text{out}}^o(\mathcal{L}_{\text{out}})$ , a MAP decision is performed to determine the most likely error coset  $\tilde{\mathcal{L}}_{\text{out}}$ , which is then used by the recovery operation  $\mathcal{R}$  to yield the estimated logical qubits  $|\tilde{\psi}_{\text{out}}\rangle$ . The *a posteriori* and extrinsic information outputs from both the SISO decoder  $D_{\text{in}}$  and  $D_{\text{out}}$  are computed using the degenerate MAP algorithm [8], [11].

## B. QBER PERFORMANCE EVALUATION

A rate-1/9 QTC consisting of two serially concatenated identical rate-1/3, memory-3 [3,1,3] QCCs is considered in all our simulations throughout this paper. More explicitly, the [3,1,3] QCC employed as both the outer and inner component codes correspond to the code configuration termed as “PTO1R” in [10].<sup>2</sup> The seed transformation for the “PTO1R” configuration in decimal notation is given by [10]:

$$U = \{1355, 2847, 558, 2107, 3330, 739, 2009, 286, 473, 1669, 1979, 189\}_{10}, \quad (9)$$

and we define the overall configuration of the QTC as “PTO1R-PTO1R” where the first and second “PTO1R” terms correspond to the “PTO1R” configuration employed by the outer code and inner code, respectively.

<sup>2</sup>The “PTO1R” term was denoted in [10] referring to the first code configuration suggested in [8] by D. Poulin (“P”), J-P. Tillich (“T”) and H. Ollivier (“O”).

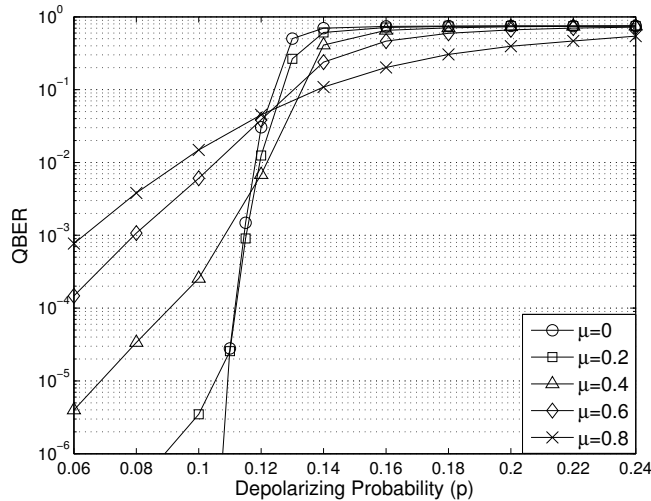


FIGURE 4: QBER performance of the rate-1/9 QTC (using the “PTO1R-PTO1R” configuration of [10]) transmitted over depolarizing channels associated with different  $\mu$  for a maximum of 8 iterations and an interleaving depth of  $3 \times 10^3$  qubits.

The qubit error rate (QBER) performance of the existing QTC in the face of depolarizing channels associated with different  $\mu$  is depicted in Fig. 4. The performance of the existing QTC is slightly improved for a higher  $\mu$  value, but only in the high  $p$ -value region, for example for  $p > 0.14$  in Fig. 4. On the other hand, in the low  $p$ -value region, we can see that the performance of the existing QTC is degraded upon increasing the  $\mu$  value. If we consider the QBER of  $10^{-6}$ , the existing QTC encountering the memoryless channels ( $\mu = 0$ ) has the best performance. However, the existing QTC does not seem to work well for channels exhibiting memory ( $\mu > 0$ ), since the performance of the existing QTC becomes worse for higher values of  $\mu$ . This is expected due to the assumption of  $\mu = 0$  used in existing QTCs and as the actual  $\mu$  deviates away from 0, the performance degradation of existing QTCs becomes more significant. Therefore, a new QTC-based coding scheme has to be designed for exploiting the error-correlation characterized by different values of  $\mu$ .

#### IV. QUANTUM TURBO CODING DESIGN EXPLOITING THE ERROR-CORRELATION

In Section II-B, it was shown that the capacity of the depolarizing channels increases with  $\mu$ . However, the results of Fig. 4 suggest that the existing QTCs encountering a channel exhibiting memory perform worse than over the memoryless channel especially for channels associated with a higher value of  $\mu$ . Therefore, a new quantum turbo coding scheme known as QTC-EEC is conceived for exploiting the error-correlation imposed by the channel and for circumventing the performance degradation exhibited by the existing QTCs. The proposed QTC-EEC relies on the appropriate modification of the MAP algorithm employed by the inner decoder to incorporate the memory state of the previous error. In this

section, we shall first present the modified MAP algorithm, followed by its EXIT chart analysis and by the performance evaluation of the proposed QTC-EEC.

#### A. MODIFIED MAP ALGORITHM CONCEIVED FOR EXPLOITING THE ERROR-CORRELATION

The degenerate MAP algorithm [8], [11] employed for the existing QTC assumes that the quantum channels are memoryless. In order to exploit the memory of the depolarizing channels, the algorithm employed by the inner decoder has to be modified. Based on the Markovian correlated-error model described in Section II-A, the Markov state of the previous error can be incorporated into the existing trellis states of the QCC and this results in an increase of the total number of trellis states from  $4^{m_{in}}$  to  $4^{m_{in}+1}$  states. The modified MAP algorithm is based on this trellis expansion, which is the price paid for exploiting the correlation  $\mu$  for the computation of the *a posteriori* probabilities.

The correlated errors of depolarizing channels with memory can be characterized by the transition probabilities given in Eq. (4), which depend on the value of the depolarizing probability  $p$  and on the correlation parameter  $\mu$ . We will exploit these transition probabilities in our modified MAP algorithm and since the transition probabilities have already included  $p$ , we can omit the contribution from the channel’s output information  $P_{ch}$ . Instead, we include it along with the transition probabilities  $q_{A|A'}$  in the modified MAP algorithm, where  $A'$  and  $A$  are the binary-representations of the Pauli operators  $\mathcal{A}'$  and  $\mathcal{A}$ , respectively and  $\{A', A\} \in G_1$ .<sup>3</sup> In the proposed QTC-EEC, the modified MAP algorithm is only employed by the inner SISO decoder  $D_{in}$ , while the outer SISO decoder  $D_{out}$  still employs the original degenerate MAP algorithm [8], [11]. The modification of the degenerate MAP algorithm is based on a similar technique of modifying the MAP algorithm for correlated binary sources in the classical domain [45]–[47].

The degenerate MAP algorithm is executed in the classic domain, hence we will replace the Pauli operators  $\mathcal{P}$ ,  $\mathcal{L}$ ,  $\mathcal{S}$  and  $\mathcal{G}$  by the classic binary-representation  $P$ ,  $L$ ,  $S$ , and  $G$ , respectively using the Pauli-to-binary isomorphism, which maps each qubit onto two classical bits [8], [11]. For the sake of generalization, we will omit the subscript ‘in’ and ‘out’ whenever our discussions apply for both the inner and outer decoders throughout the following discussions. For a sequence of  $T$  blocks of  $k$  logical qubits (correspondingly,  $n$  physical qubits),<sup>4</sup> let  $L = [L_1, L_2, \dots, L_t, \dots, L_T]$  and  $P = [P_1, P_2, \dots, P_t, \dots, P_T]$  where  $L_t \in G_k$  and  $P_t \in G_n$ . More explicitly,  $L_t = [L_t^1, L_t^2, \dots, L_t^k]$  and  $P_t = [P_t^1, P_t^2, \dots, P_t^n]$ . Based on the circuit representation of a QCC [11], we have

$$(M_t : P_t) = (M_{t-1} : L_t : S_t)U, \quad (10)$$

<sup>3</sup>Since  $A'$  and  $A$  are the binary-representation of Pauli operators  $\mathcal{A}'$  and  $\mathcal{A}$ , respectively, we have  $q_{A|A'} = q_{\mathcal{A}|\mathcal{A}'}$  and similarly,  $p_A = p_{\mathcal{A}}$  for  $\{\mathcal{A}', \mathcal{A}\} \in G_1$ .

<sup>4</sup>The  $T$  number of blocks may include the block(s) of terminated qubits.

where the colon (:) represents the concatenation operation,  $U$  is the  $2(n+m) \times 2(n+m)$  seed transformation matrix and  $M \in G_m$  is the memory state having a length of  $2m$  bits. The seed transformation  $U$  can be decomposed as  $U = (U_M : U_P)$ , where  $U_M$  and  $U_P$  are binary matrices constructed by the first  $2m$  columns and the last  $2n$  columns of  $U$ , respectively. Hence, we have

$$M_t = (M_{t-1} : L_t : S_t)U_M, \quad (11)$$

$$P_t = (M_{t-1}, L_t : S_t)U_P. \quad (12)$$

We have derived the *a posteriori* probabilities,  $P^o(L_{in,t})$  and  $P^o(P_{in,t})$  using the modified degenerate MAP algorithm as follows:

$$\begin{aligned} P^o(L_{in,t}) &\triangleq P(L_{in,t} | S_{in,t}^x), \\ &\propto \sum_{\nu, \lambda, \sigma, \xi} P^a(L_{in,t}) \cdot \alpha_{t-1}(\nu, \xi) \cdot \beta_t(M_{in,t}, P_{in,t}^{n_{in}}) \\ &\quad \cdot q_{P_{in,t}^1 | \xi} \cdot \prod_{j=2}^{n_{in}} q_{P_{in,t}^j | P_{in,t}^{j-1}} \end{aligned} \quad (13)$$

and

$$\begin{aligned} P^o(P_{in,t}) &\triangleq P(P_{in,t} | S_{in,t}^x), \\ &\propto \sum_{\nu, \lambda, \sigma, \xi} P^a(L_{in,t} = \lambda) \cdot \alpha_{t-1}(\nu, \xi) \cdot \beta_t(M_{in,t}, P_{in,t}^{n_{in}}) \\ &\quad \cdot q_{P_{in,t}^1 | \xi} \cdot \prod_{j=2}^{n_{in}} q_{P_{in,t}^j | P_{in,t}^{j-1}}, \end{aligned} \quad (14)$$

where  $\nu \in G_m$ ,  $\lambda \in G_k$ ,  $\sigma \in G_{n-k}$  and  $\xi \in G_1$ , while  $\sigma = (\sigma_x : \sigma_z)$  having  $\sigma_x = S_t^x$ . The variable  $\xi$  corresponds to all possible errors imposed on the  $n_{in}$ -th qubit at time instant  $t-1$ , i.e.  $P_{in,t-1}^{n_{in}} = \xi$ . Based on Eq. (11) and Eq. (12), we have  $M_{in,t} = (\nu : L_{in,t} : \sigma)U_M$  and  $P_{in,t} = (\nu : L_{in,t} : \sigma)U_P$ , where  $P_{in,t} = [P_{in,t}^1, P_{in,t}^2, \dots, P_{in,t}^{n_{in}}]$  and  $L_{in,t} = [L_{in,t}^1, L_{in,t}^2, \dots, L_{in,t}^{n_{in}}]$ . The  $\propto$  sign indicates that the left-hand-side term is proportional to the corresponding right-hand side term, with the proportionality factor for a fixed  $t$  being given by normalization. This ensures that for a fixed  $t$ , the sum of probabilities of the left-hand-side term, e.g.,  $P^o(L_{in,t})$  in Eq. (13) and  $P^o(P_{in,t})$  in Eq. (14) is always equal to 1.

The forward recursive coefficient  $\alpha_t$  and the backward recursive coefficient  $\beta_{t-1}$  are formulated as:

$$\begin{aligned} \alpha_t(M_{in,t}, P_{in,t}^{n_{in}}) &\triangleq P(M_{in,t}, P_{in,t}^{n_{in}} | S_{in,t}^x), \\ &\propto \sum_{\nu, \lambda, \sigma, \xi} P^a(L_{in,t} = \lambda) \cdot \alpha_{t-1}(\nu, \xi) \cdot q_{P_{in,t}^1 | \xi} \cdot \prod_{j=2}^{n_{in}} q_{P_{in,t}^j | P_{in,t}^{j-1}} \end{aligned} \quad (15)$$

and

$$\begin{aligned} \beta_{t-1}(M_{in,t-1}, P_{in,t-1}^{n_{in}}) &\triangleq P(M_{in,t-1}, P_{in,t-1}^{n_{in}} | S_{in,t-1}^x), \\ &\propto \sum_{\lambda, \sigma} P^a(L_{in,t} = \lambda) \cdot \beta_t(M_{in,t}, P_{in,t}^{n_{in}}) \cdot q_{P_{in,t}^1 | P_{in,t-1}^{n_{in}}} \\ &\quad \cdot \prod_{j=2}^{n_{in}} q_{P_{in,t}^j | P_{in,t}^{j-1}}, \end{aligned} \quad (16)$$

respectively, where  $M_{in,t} = (M_{in,t-1} : \lambda : \sigma)U_M$  and  $P_{in,t} = (M_{in,t-1} : \lambda : \sigma)U_P$ .

The boundary conditions for  $\alpha_t$  at  $t = 0$  and  $\beta_t$  at  $t = T_{in}$  can be computed as:

$$\alpha_0(M_{in,0} = \gamma, P_{in,0}^{n_{in}} = A) = \begin{cases} \frac{p_A}{2^m}, & \text{if } \gamma^x = S_{in,0}^x \\ 0, & \text{if } \gamma^x \neq S_{in,0}^x \end{cases} \quad (17)$$

and

$$\beta_{T_{in}}(M_{in,T_{in}} = \gamma, P_{in,T_{in}}^{n_{in}} = A) = q_{\gamma^1 | A} \cdot \prod_{j=2}^{m_{in}} q_{\gamma^j | \gamma^{j-1}}, \quad (18)$$

respectively, where  $A \in G_1$ ,  $\gamma \in G_m$  and  $\gamma^x$  is the  $\mathbf{X}$ -component of  $\gamma$ .

The marginal *a posteriori* probabilities  $P^o(L_{in,t}^j)$  for  $j \in \{1, \dots, k\}$  and  $P^o(P_{in,t}^j)$  for  $j \in \{1, \dots, n\}$  are then computed from  $P^o(L_{in,t})$  and  $P^o(P_{in,t})$ , respectively. The marginal extrinsic probabilities  $P^e(L_{in,t}^j)$  for  $j \in \{1, \dots, k\}$  and  $P^e(P_{in,t}^j)$  for  $j \in \{1, \dots, n\}$  can then be computed by taking out the *a priori* information from the resultant *a posteriori* information, i.e. we have

$$P^e(L_{in,t}^j) \propto \frac{P^o(L_{in,t}^j)}{P^a(L_{in,t}^j)}, \quad (19)$$

$$P^e(P_{in,t}^j) \propto \frac{P^o(P_{in,t}^j)}{P^a(P_{in,t}^j)}. \quad (20)$$

It is worth noting that at  $\mu = 0$  (memoryless channels), we have  $q_{A|A'} = p_A$  for  $\{A', A\} \in G_1$  and hence, the term  $q_{P_{in,t}^1 | \xi} \prod_{j=2}^{n_{in}} q_{P_{in,t}^j | P_{in,t}^{j-1}}$  in Eq. (13), Eq. (14) and Eq. (15) can be simplified to

$$\begin{aligned} q_{P_{in,t}^1 | \xi} \cdot \prod_{j=2}^{n_{in}} q_{P_{in,t}^j | P_{in,t}^{j-1}} &= \prod_{j=1}^{n_{in}} p_{P_{in,t}^j} \\ &= P^a(P_{in,t}), \end{aligned} \quad (21)$$

and similarly in Eq. (16),

$$\begin{aligned} q_{P_{in,t}^1 | P_{in,t-1}^{n_{in}}} \cdot \prod_{j=2}^{n_{in}} q_{P_{in,t}^j | P_{in,t}^{j-1}} &= \prod_{j=1}^{n_{in}} p_{P_{in,t}^j} \\ &= P^a(P_{in,t}). \end{aligned} \quad (22)$$

Therefore, the computation of the *a posteriori* probabilities using the modified degenerate MAP algorithm is equivalent to the computation of the *a posteriori* probabilities using the original degenerate MAP algorithm [8], [11] at  $\mu = 0$ .

### B. EXIT CHART ANALYSIS AND QBER PERFORMANCE EVALUATION

EXIT-charts constitute an essential tool that has been widely used for the design of near-capacity classical codes as a benefit of its capability of visualizing the convergence behavior of iterative decoding schemes [48], [49]. The classical non-binary EXIT chart technique of [50], [51] was adapted to the quantum syndrome decoding approach in [12] which was realized by exploiting the equivalent classical representation of the quantum code and based on the analogy of the memoryless depolarizing channel with the binary symmetric channel. The EXIT chart conceived for the quantum domain models the *a priori* information related to the error-sequence imposed on the logical qubits (or physical qubits), unlike its classical counterpart where the *a priori* information concerning the uncoded (or encoded) bits is modeled.

In this treatise we adopt the quantum-domain EXIT charts [12] to evaluate the EXIT characteristics of the inner SISO decoder  $D_{\text{in}}$  and of the outer SISO decoder  $D_{\text{out}}$  in Fig. 3 for depolarizing channels with memory. There are four information terms involved in the exchange of information between  $D_{\text{in}}$  and  $D_{\text{out}}$  and the information is given in terms of the average mutual information (MI) for the EXIT chart analysis. The four information quantities involved are the average *a priori* MI of  $D_{\text{in}}$  corresponding to  $L_{\text{in}}$  denoted as  $I_a(L_{\text{in}})$ , the average extrinsic MI of  $D_{\text{in}}$  corresponding to  $L_{\text{in}}$  denoted as  $I_e(L_{\text{in}})$ , the average *a priori* MI of  $D_{\text{out}}$  corresponding to  $P_{\text{out}}$  denoted as  $I_a(P_{\text{out}})$  and lastly, the average extrinsic MI of  $D_{\text{out}}$  corresponding to  $P_{\text{out}}$  denoted as  $I_e(P_{\text{out}})$ . The EXIT-functions  $\mathcal{T}_{\text{in}}$  for  $D_{\text{in}}$  and  $\mathcal{T}_{\text{out}}$  for  $D_{\text{out}}$  are given by

$$I_e(L_{\text{in}}) = \mathcal{T}_{\text{in}}(I_a(L_{\text{in}}), p, \mu) \quad (23)$$

and

$$I_e(P_{\text{out}}) = \mathcal{T}_{\text{out}}(I_a(P_{\text{out}})), \quad (24)$$

respectively. The value of  $I_e(L_{\text{in}})$  is affected not only by the  $I_a(L_{\text{in}})$  value but also by the depolarizing probability  $p$  and by the Markovian correlation  $\mu$  of the depolarizing channel exhibiting memory. Meanwhile, the value of  $I_e(P_{\text{out}})$  depends only on the value of  $I_a(P_{\text{out}})$ .

The EXIT curves of the inner SISO decoder employing the original MAP algorithm (for QTC) and the modified MAP algorithm (for QTC-EEC) for transmission over depolarizing channels having different  $\mu$  values are portrayed in Fig. 5. It can be observed that as the channels exhibiting stronger error-correlation, the EXIT curves of the QTC emerge from a higher  $I_e(L_{\text{in}})$  value at  $I_a(L_{\text{in}}) = 0$  and terminated at a lower

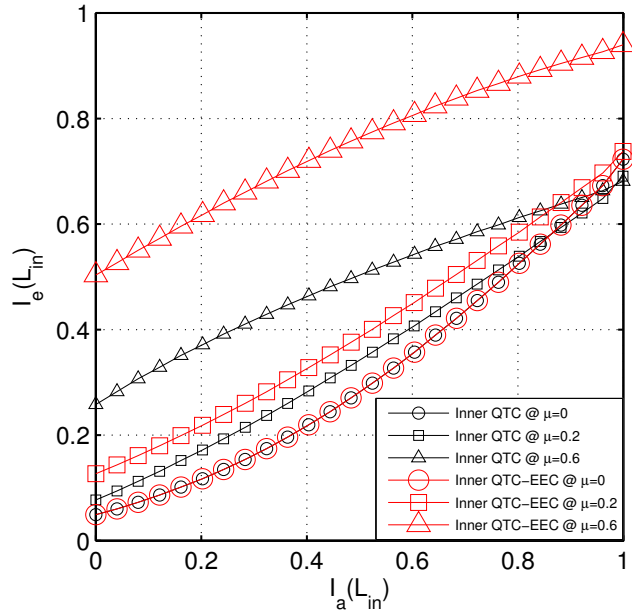


FIGURE 5: EXIT curves of the inner decoder of the existing QTC and the proposed QTC-EEC for the “PTO1R” configuration of [10] for transmission over depolarizing channels having different  $\mu$  evaluated at  $p = 0.23$ .

$I_e(L_{\text{in}})$  value at  $I_a(L_{\text{in}}) = 1$ .<sup>5</sup> On the other hand, extrinsic MI  $I_e(L_{\text{in}})$  gains are observed for the QTC-EEC across all  $I_a(L_{\text{in}})$  values, as  $\mu$  increases. The proposed QTC-EEC using the modified MAP algorithm achieves higher extrinsic MI  $I_e(L_{\text{in}})$  values than the existing QTC that uses the original MAP algorithm for  $\mu > 0$ . At  $\mu = 0$ , our proposed inner decoder (QTC-EEC) has identical EXIT curves to the existing inner decoder (QTC)<sup>6</sup> since our modified MAP algorithm is simplified to the original MAP algorithm at  $\mu = 0$ . The  $I_e(L_{\text{in}})$  gains achieved by our proposed inner decoder (QTC-EEC) over the existing inner decoder (QTC) would improve the decoding convergence threshold at a higher depolarizing probability  $p$ .

Fig. 6 shows the matching between the EXIT curves of the proposed inner decoder at different  $p$  values and of the outer decoder for a depolarizing channel associated with  $\mu = 0.6$ . It can be deduced from Fig. 6 that the convergence threshold  $p^E$  is at  $p = 0.225$ , since the tunnel between the curves corresponding to the inner and outer decoders is marginally open at this point and increasing  $p$  beyond  $p = 0.225$ , to say  $p = 0.23$  closes the EXIT tunnel. Fig. 6 also depicts two snapshot decoding trajectories at  $p = 0.225$  using an

<sup>5</sup>It was found in [7] that the QCCs without pre-shared entanglement cannot be simultaneously recursive and non-catastrophic. All QCCs including the “PTO1R” code have non-recursive and non-catastrophic properties. Hence, QTCs with a QCC as the inner code have a bounded minimum distance and the EXIT curve for the inner decoder is only capable to reach  $(x, y) = (1, 1)$  point at very low values of  $p$ , whereas the classical recursive inner codes can reach  $(x, y) = (1, 1)$  point for any  $p$  value [12].

<sup>6</sup>In the simulations, we deliberately used the same samples for both decoders to show the similarity of both decoders at  $\mu = 0$ .

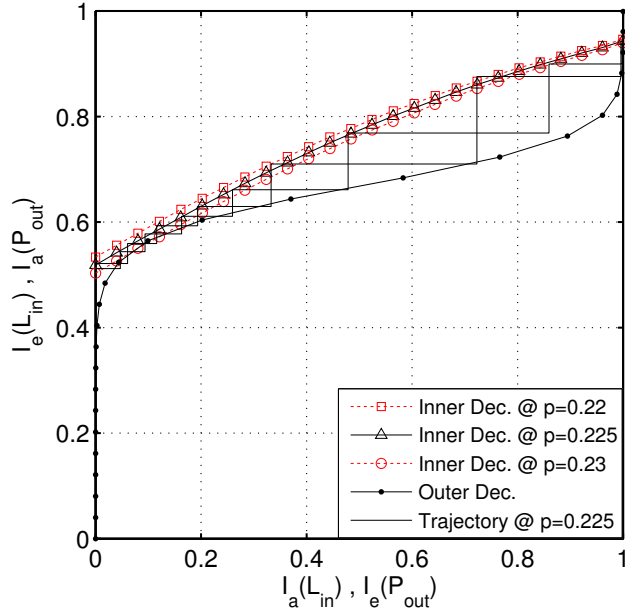


FIGURE 6: EXIT chart and two snapshot decoding trajectories of the rate-1/9 QTC-EEC for the “PTO1R-PTO1R” configuration of [10] transmitted over depolarizing channels having  $\mu = 0.6$ . An interleaving depth of  $3 \times 10^4$  qubits was used.

TABLE 1: Distance to capacity for the QTC-EEC over depolarizing channels having  $\mu = \{0, 0.2, 0.6\}$

Correlation parameter, $\mu$	0	0.2	0.6
Convergence threshold, $p^E$	0.125	0.135	0.225
Noise limit, $p^*$	0.160	0.175	0.297
Distance-to-limit, $p^E/p^*$	0.78	0.77	0.76

interleaver length of  $3 \times 10^4$  qubits. The trajectories are based on the actual performance and it can be seen in Fig. 6 that the trajectories are well-matched with the corresponding EXIT curves. Therefore, the accuracy of our EXIT chart predictions is verified.

The convergence threshold  $p^E$  at  $\mu = 0$  and  $\mu = 0.2$  is given in Table 1. The noise limit  $p^*$  for  $\mu = \{0, 0.2, 0.6\}$  is obtained from the corresponding capacity curve seen in Fig. 2. The distance from the limit given as  $p^E/p^*$  [37] is then determined as tabulated in Table 1 for the depolarizing channels associated with  $\mu = \{0, 0.2, 0.6\}$ . The memoryless channel at  $\mu = 0$  has the shortest distance from the limit, which is 0.78 and the distance from the limit for  $\mu = 0.2$  and  $\mu = 0.6$  is not far from that of the memoryless channel scenario associated with the distance of 0.77 and 0.76, respectively. The “PTO1R” configuration was specifically designed for memoryless channels in [8], [10]. This suggests that the performance of the proposed QTC-EEC can be potentially improved by using different code configurations in order to approach the capacity limit. The search for the optimal inner and outer component codes of the QTC-EEC for different  $\mu$  values remains an open problem for future investigations.

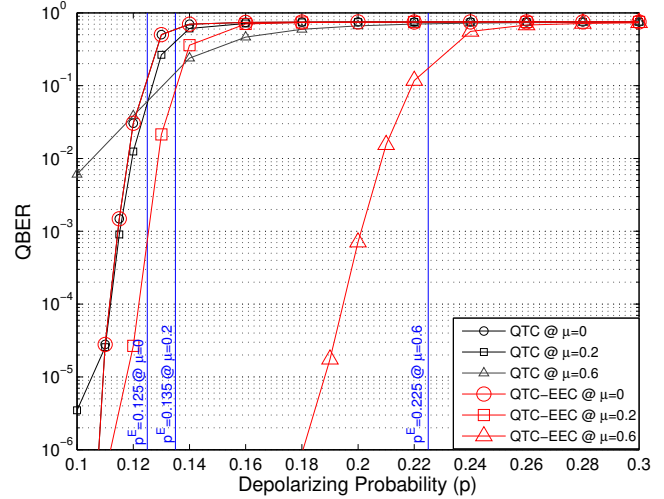


FIGURE 7: QBER performance of the rate-1/9 existing QTC and of the proposed QTC-EEC for transmission over depolarizing channels exhibiting memory relying on the “PTO1R-PTO1R” configuration of [10] for a maximum of 8 iterations and an interleaving depth of  $3 \times 10^3$  qubits.

The QBER performance of the proposed QTC-EEC in the face of depolarizing channels associated with  $\mu = \{0, 0.2, 0.6\}$  is depicted in Fig. 7. The turbo-cliff region starts around the  $p = p^E$  ( $p^E$  value, as seen in Table 1), since a rapid QBER drop can be observed as  $p$  decreases beyond  $p = p^E$ . Therefore, our EXIT chart predictions are consistent with the QBER simulation results. The performance curves can be improved to closely approach  $p = p^E$  by increasing the number of iterations and by using higher interleaving depths [48]. Fig. 7 also compares the performance of the proposed QTC-EEC to that of the existing QTC at  $\mu = \{0, 0.2, 0.6\}$ . We have deliberately used the same set of samples for the QTC-EEC at  $\mu = 0$  to demonstrate that the same performance is achieved at  $\mu = 0$  as that of the existing QTC. As  $\mu$  increases, we can observe the performance degradation of the existing QTC especially in the error-floor region, whereas, the performance of QTC-EEC is significantly improved and better performance gains were achieved than by the existing QTC at  $\mu = 0$ .

Fig. 8 compares the QBER performance between the proposed QTC-EEC and the QTC relying on the Markov decoder (QTC-MD) at  $\mu = 0.2$  and 0.6. The QTC-MD scheme is a three-stage serially concatenated decoding scheme consisting of two component decoders of the existing QTC, where a Markov decoder is invoked for exploiting the error-correlation. The Markov decoder is based on the MAP algorithm designed for the classical soft-bit source decoding in [52], [53], but here we consider the soft decoding benefits of error-correlation instead of source-correlation. The proposed QTC-EEC has an increased computational complexity as the number of trellis states at the inner decoder is expanded by a factor of 4 compared to the existing QTC, i.e., from  $4^{m_{in}}$  to

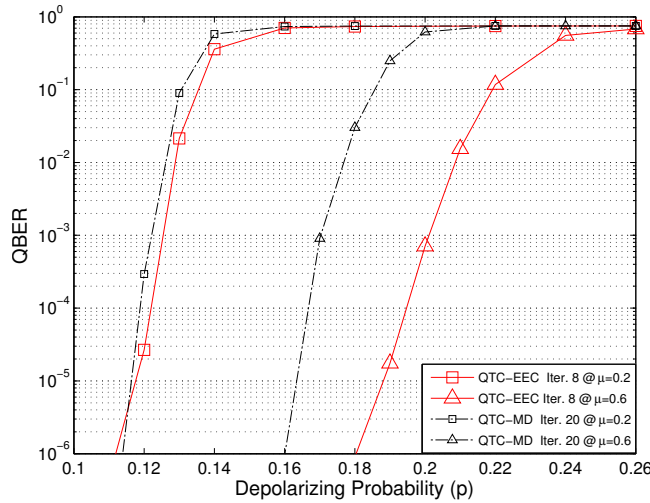


FIGURE 8: QBER performance of the proposed QTC-EEC and of the QTC-MD for transmission over depolarizing channels exhibiting memory relying on the “PTO1R-PTO1R” configuration of [10] having a coding rate of 1/9 and an interleaving depth of  $3 \times 10^3$  qubits.

$4^{m_{in}+1}$  trellis states, where we have  $m_{in} = 3$  for the “PTO1R” configuration. The decoding complexity is proportional to the product of the total number of trellis states (both component decoders) and the number of iterations. Therefore, the QTC-EEC associated with 8 iterations has a complexity proportional to  $(4^3 + 4^4) \times 8 = 2560$ . For the sake of a fair comparison in terms of the complexity, 20 iterations are invoked for the existing QTC (resulting in a complexity of  $\propto (4^3 + 4^3) \times 20 = 2560$ ) and the QTC-MD (resulting in a complexity  $\propto (4^3 + 4^3 + 4) \times 20 = 2640$ ). It can be observed that at a QBER of  $10^{-4}$ , the proposed QTC-EEC outperforms the QTC-MD schemes for depolarizing channels associated with  $\mu = 0.2$  and  $0.6$ .

## V. JOINT DECODING AND ESTIMATION OF THE CORRELATION PARAMETER

In the previous section, we have shown the efficiency of the proposed QTC-EEC in exploiting the error-correlation from quantum channels exhibiting memory given, that we have the knowledge of  $\mu$ . However, the value of  $\mu$  is unknown in practical communication systems and it may vary from one transmission to another, depending on the condition of the channel at the point of the transmission. In this section, we propose a joint decoding and estimation scheme termed as QTC-EEC-E for the simultaneous estimation of  $\mu$  while performing the iterative decoding.

The estimation is performed every time the modified MAP algorithm employed by the inner decoder is activated. Before invoking iterative decoding, we assume that the initial value of  $\mu$  is given by  $\hat{\mu}_{ini} = 0.5$ . The error imposed on the physical qubits of the inner code is given by  $P_{in} = [P_{in,1}, P_{in,2}, \dots, P_{in,t}, \dots, P_{in,T_{in}}]$  where we have  $P_{in,t} = [P_{in,t}^1, P_{in,t}^2, \dots, P_{in,t}^j, \dots, P_{in,t}^{n_{in}}]$ . Hence the total num-

ber of qubits transmitted for the whole frame is  $N = T_{in} \times n_{in}$ , which corresponds to  $N$  channel uses. The error imposed on the  $j$ -th qubit at time instant  $t$  of  $P_{in}$ , i.e.  $P_{in,t}^j$  corresponds to the error corrupting the  $(n_{in}(t-1) + j)$ -th qubit of the whole frame. Therefore, we denote  $P_{in,t}^j$  as  $A_{n_{in}(t-1)+j}$  and can alternatively represent  $P_{in}$  as  $P_{in} = [A_1, A_2, \dots, A_i, \dots, A_N]$ , where we have  $i = n_{in}(t-1) + j$ .

The procedure of estimating the correlation parameter  $\mu$  is as follows:

- **Step-1:** Compute the joint *a posteriori* probability  $P^o(A_{i-1} = A', A_i = A)$  for  $\{A', A\} \in G_1$  and  $i \in \{2, 3, \dots, N\}$ . This can be carried out by computing the joint *a posteriori* probability  $P^o(P_{in,t-1}^{n_{in}}, P_{in,t})$  from Eq. (14) (used in the modified MAP algorithm) as follows:

$$\begin{aligned} P^o(P_{in,t-1}^{n_{in}} = A', P_{in,t}) &\triangleq P(P_{in,t-1}^{n_{in}} = A', P_{in,t} | S_{in,t}^x), \\ &\propto \sum_{\nu, \lambda, \sigma} P^a(L_{in,t} = \lambda) \cdot \alpha_{t-1}(\nu, A') \cdot \beta_t(M_{in,t}, P_{in,t}^{n_{in}}) \\ &\quad \cdot q_{P_{in,t}^1 | A'} \cdot \prod_{j=2}^{n_{in}} q_{P_{in,t}^j | P_{in,t}^{j-1}}. \end{aligned} \quad (25)$$

Let us now represent  $P^o(P_{in,t-1}^{n_{in}}, P_{in,t})$  as

$$P^o(A_{n_{in}(t-1)}, A_{n_{in}(t-1)+1}, A_{n_{in}(t-1)+2}, \dots, A_{n_{in}(t-1)+n_{in}}). \quad (26)$$

We can then obtain the marginal probabilities  $P^o(A_{n_{in}(t-1)}, A_{n_{in}(t-1)+1}), P^o(A_{n_{in}(t-1)+1}, A_{n_{in}(t-1)+2}), \dots$ , and  $P^o(A_{n_{in}(t-1)+n_{in}-1}, A_{n_{in}(t-1)+n_{in}})$  from Eq. (26).

- **Step-2:** Find the transition probabilities  $\bar{q}_{A|A'} = P(A_i = A | A_{i-1} = A')$  from the *a posteriori* probabilities using

$$\bar{q}_{A|A'} = \frac{\sum_{i=2}^N P^o(A_{i-1} = A', A_i = A)}{\sum_{i=2}^N P^o(A_{i-1} = A')}. \quad (27)$$

- **Step-3:** The relationship of  $q_{A|A'}$  and the correlation parameter  $\mu$  is given by  $q_{A|A'} = (1 - \mu)p_A + \mu\delta_{A'A}$ . Hence, the correlation parameter  $\hat{\mu}_{A'A}$  that corresponds to each  $\bar{q}_{A|A'}$  can be expressed as follows:

$$\hat{\mu}_{A'A} = \begin{cases} \frac{\bar{q}_{A|A'} - p_A}{1 - p_A}, & \text{if } A' = A \\ 1 - \frac{\bar{q}_{A|A'}}{p_A}, & \text{if } A' \neq A, \end{cases} \quad (28)$$

where  $p_A$  is the probability of the Pauli operator  $A$  imposed on the transmitted qubits.

- **Step-4:** Obtain the estimated  $\hat{\mu}$  by finding the mean of the set  $\{\hat{\mu}_{A'A}\}$ . Since  $\mu \in [0, 1]$ , if  $\hat{\mu} < 0$ , then  $\hat{\mu} = 0$  and if  $\hat{\mu} > 1$ , then  $\hat{\mu} = 1$ .

- **Step-5:** Update the transition probabilities using the estimated  $\hat{\mu}$ , where the updated transition probabilities defined as  $\hat{q}_{A|A'}$  are given by  $\hat{q}_{A|A'} = (1 - \hat{\mu})p_A + \hat{\mu}\delta_{A'A}$ .

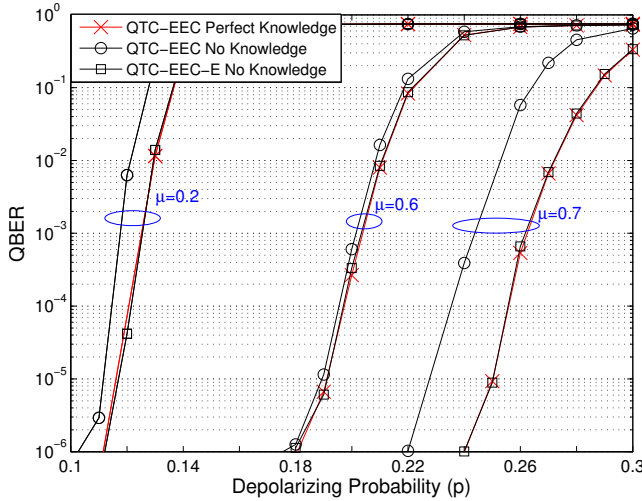


FIGURE 9: QBER performance of the QTC-EEC-E with unknown  $\mu$ , of the QTC-EEC with unknown  $\mu$  and of the ideal system of QTC-EEC with known  $\mu$  after 20 iterations. All the coding schemes rely on the “PTO1R-PTO1R” configuration of [10] having a coding rate of 1/9 and an interleaving depth of  $3 \times 10^3$  qubits.

The inner SISO decoder will then use the updated transition probabilities  $\hat{q}_{A|A'}$ , when invoking the MAP decoding during the next iteration.

- **Step-6:** Step-1 to Step-5 is repeated at every iteration to re-estimate  $\hat{\mu}$  and correspondingly,  $\hat{q}_{A|A'}$ .

The performance comparison when  $\mu$  is unknown between the QTC-EEC-E and QTC-EEC ( $\mu = 0.5$  is assumed) for transmission over depolarizing channels associated with  $\mu = \{0.2, 0.6, 0.7\}$  after 20 iterations is portrayed in Fig. 9. The superiority of the QTC-EEC-E is demonstrated, since we can observe that the QTC-EEC-E equipped with the estimation capability outperforms the QTC-EEC having no estimation capability for all the evaluated cases, when the knowledge of  $\mu$  is not available at the receiver. Since the QTC-EEC always assumes  $\mu = 0.5$  regardless of the actual  $\mu$  value, the performance gap between the QTC-EEC-E and QTC-EEC becomes more significant, when the actual  $\mu$  of the channel is further away from  $\mu = 0.5$ . Moreover, it can be observed that there is almost no performance loss between the QTC-EEC-E with unknown  $\mu$  and the ideal system of QTC-EEC with known  $\mu$ . Therefore, a near-perfect estimation using the proposed QTC-EEC-E is demonstrated.

Fig. 10 shows the QBER performance of both the QTC-EEC-E (with unknown  $\mu$ ) and of the QTC-EEC (with known  $\mu$ ) as a function of the number of iterations at  $\mu = 0.6$ . The performance of the QTC-EEC-E converges to the QBER level of the ideal QTC-EEC having a known  $\mu$  after a number of iterations for all the evaluated cases at  $p = \{0.19, 0.20, 0.21\}$ . This suggests that the QTC-EEC-E is capable of achieving the same performance as the ideal system but it requires more iterations to reach the steady-state

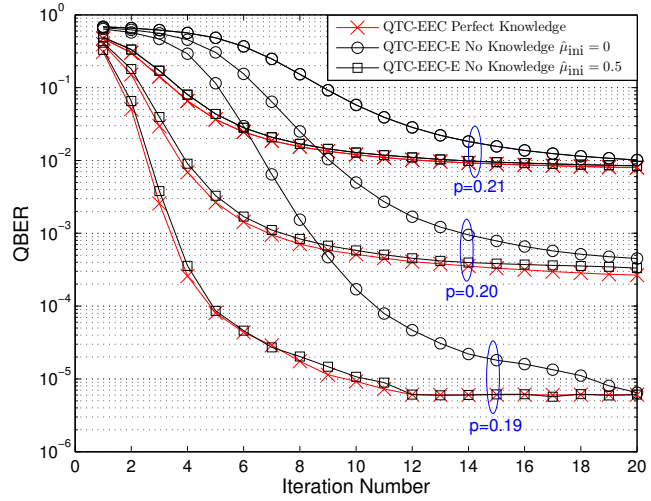


FIGURE 10: QBER as a function of the decoding iteration number for the QTC-EEC-E with unknown  $\mu$  and the ideal system of QTC-EEC with known  $\mu$  over depolarizing channels having  $\mu = 0.6$ . All the coding schemes rely on the “PTO1R-PTO1R” configuration of [10] associated with a coding rate of 1/9 and an interleaving depth of  $3 \times 10^3$  qubits.

QBER. The number of additional iterations required depends on the value of  $\hat{\mu}_{\text{ini}}$  (the initial value of  $\hat{\mu}$ ). Observe in Fig. 10 that  $\hat{\mu}_{\text{ini}} = 0.5$  can reach the steady-state of the QBER much faster than when  $\hat{\mu}_{\text{ini}} = 0$ . This is simply because  $\hat{\mu}_{\text{ini}} = 0.5$  is closer to the actual  $\mu = 0.6$  and therefore the closer the value of  $\hat{\mu}_{\text{ini}}$  to the actual  $\mu$ , the less iterations are required for reaching the steady-state of the QBER.

## VI. CONCLUSIONS

In this paper, the design of QTCs for depolarizing channels exhibiting memory has been considered. The performance of an existing QTC over depolarizing channels exhibiting memory has been investigated and it has been shown that the performance of the existing QTC in the low  $p$ -value region is degraded for channels having a higher correlation. In order to circumvent the performance degradation problem, QTC-EEC has been proposed for exploiting the error-correlation when performing iterative decoding. The proposed QTC-EEC is capable of achieving the convergence threshold at a higher depolarizing probability for channels with a higher value of the correlation parameter and furthermore, sharp turbo-cliff without significant error-floor can be seen exhibited by the proposed QTC-EEC. We have shown that the proposed QTC-EEC achieves a performance near to the capacity and outperforms the relevant benchmark systems, i.e. both the existing QTC and the QTC-MD in all the evaluated cases. For systems with unknown correlation parameter, we have conceived a joint decoding and estimation scheme based on the QTC-EEC scheme termed as QTC-EEC-E. Simulation results have revealed that the proposed QTC-EEC-E achieves the same performance as that the ideal system having perfect knowledge of the correlation parameter and hence, demon-

strate the accurate estimation of the proposed QTC-EEC-E.

## REFERENCES

- [1] S. Imre and F. Balazs, *Quantum Computing and Communications: An Engineering Approach*. John Wiley & Sons, 2005.
- [2] P. W. Shor, "Scheme for reducing decoherence in quantum computer memory," *Phys. Rev. A*, vol. 52, pp. R2493–R2496, Oct 1995. [Online]. Available: <http://link.aps.org/doi/10.1103/PhysRevA.52.R2493>
- [3] L. Viola, E. Knill, and S. Lloyd, "Dynamical decoupling of open quantum systems," *Phys. Rev. Lett.*, vol. 82, pp. 2417–2421, Mar 1999. [Online]. Available: <http://link.aps.org/doi/10.1103/PhysRevLett.82.2417>
- [4] P. Zanardi and M. Rasetti, "Noiseless quantum codes," *Phys. Rev. Lett.*, vol. 79, pp. 3306–3309, Oct 1997. [Online]. Available: <http://link.aps.org/doi/10.1103/PhysRevLett.79.3306>
- [5] D. A. Lidar, I. L. Chuang, and K. B. Whaley, "Decoherence-free subspaces for quantum computation," *Phys. Rev. Lett.*, vol. 81, pp. 2594–2597, Sep 1998. [Online]. Available: <http://link.aps.org/doi/10.1103/PhysRevLett.81.2594>
- [6] C. Berrou, A. Glavieux, and P. Thitimajshima, "Near shannon limit error-correcting coding and decoding: Turbo-codes," in *IEEE Int. Conf. Communications (ICC)*, Geneva, Switzerland, May 1993, pp. 1064–1070.
- [7] D. Poulin, J. P. Tillich, and H. Ollivier, "Quantum serial turbo-codes," in *2008 IEEE International Symposium on Information Theory*, Jul. 2008, pp. 310–314.
- [8] ———, "Quantum serial turbo codes," *IEEE Trans. Inform. Theory*, vol. 55, no. 6, pp. 2776–2798, Jun. 2009.
- [9] M. M. Wilde and M. H. Hsieh, "Entanglement boosts quantum turbo codes," in *2011 IEEE International Symposium on Information Theory Proceedings*, Jul. 2011, pp. 445–449.
- [10] M. M. Wilde, M. H. Hsieh, and Z. Babar, "Entanglement-assisted quantum turbo codes," *IEEE Trans. Inform. Theory*, vol. 60, no. 2, pp. 1203–1222, Feb. 2014.
- [11] Z. Babar, P. Botsinis, D. Alanis, S. X. Ng, and L. Hanzo, "The road from classical to quantum codes: A hashing bound approaching design procedure," *IEEE Access*, vol. 3, pp. 146–176, 2015.
- [12] Z. Babar, S. X. Ng, and L. Hanzo, "EXIT-chart-aided near-capacity quantum turbo code design," *IEEE Trans. Veh. Technol.*, vol. 64, no. 3, pp. 866–875, Mar. 2015.
- [13] M. S. Postol, "A proposed quantum low density parity check code," 2001.
- [14] D. J. C. MacKay, G. Mitchison, and P. L. McFadden, "Sparse-graph codes for quantum error correction," *IEEE Trans. Inform. Theory*, vol. 50, no. 10, pp. 2315–2330, Oct. 2004.
- [15] T. Camara, H. Ollivier, and J. P. Tillich, "A class of quantum ldpc codes: construction and performances under iterative decoding," in *2007 IEEE International Symposium on Information Theory*, Jun. 2007, pp. 811–815.
- [16] F. Caruso, V. Giovannetti, C. Lupo, and S. Mancini, "Quantum channels and memory effects," *Rev. Mod. Phys.*, vol. 86, pp. 1203–1259, Dec 2014. [Online]. Available: <http://link.aps.org/doi/10.1103/RevModPhys.86.1203>
- [17] D. Kretschmann and R. F. Werner, "Quantum channels with memory," *Phys. Rev. A*, vol. 72, p. 062323, Dec 2005. [Online]. Available: <http://link.aps.org/doi/10.1103/PhysRevA.72.062323>
- [18] S. Bose, "Quantum communication through an unmodulated spin chain," *Phys. Rev. Lett.*, vol. 91, p. 207901, Nov 2003. [Online]. Available: <http://link.aps.org/doi/10.1103/PhysRevLett.91.207901>
- [19] A. Bayat, D. Burgarth, S. Mancini, and S. Bose, "Memory effects in spin-chain channels for information transmission," *Phys. Rev. A*, vol. 77, p. 050306, May 2008. [Online]. Available: <http://link.aps.org/doi/10.1103/PhysRevA.77.050306>
- [20] G. Benenti, A. D'Arrigo, and G. Falci, "Enhancement of transmission rates in quantum memory channels with damping," *Phys. Rev. Lett.*, vol. 103, p. 020502, Jul 2009. [Online]. Available: <http://link.aps.org/doi/10.1103/PhysRevLett.103.020502>
- [21] J. Ball, A. Dragan, and K. Banaszek, "Exploiting entanglement in communication channels with correlated noise," *Phys. Rev. A*, vol. 69, p. 042324, Apr 2004. [Online]. Available: <http://link.aps.org/doi/10.1103/PhysRevA.69.042324>
- [22] K. Banaszek, A. Dragan, W. Wasilewski, and C. Radzewicz, "Experimental demonstration of entanglement-enhanced classical communication over a quantum channel with correlated noise," *Phys. Rev. Lett.*, vol. 92, p. 257901, Jun 2004. [Online]. Available: <http://link.aps.org/doi/10.1103/PhysRevLett.92.257901>
- [23] C. Macchiavello and G. M. Palma, "Entanglement-enhanced information transmission over a quantum channel with correlated noise," *Phys. Rev. A*, vol. 65, p. 050301, Apr 2002. [Online]. Available: <http://link.aps.org/doi/10.1103/PhysRevA.65.050301>
- [24] C. Macchiavello, G. M. Palma, and S. Virmani, "Transition behavior in the channel capacity of two-qubit channels with memory," *Phys. Rev. A*, vol. 69, p. 010303, Jan 2004. [Online]. Available: <http://link.aps.org/doi/10.1103/PhysRevA.69.010303>
- [25] D. Daems, "Entanglement-enhanced transmission of classical information in pauli channels with memory: Exact solution," *Phys. Rev. A*, vol. 76, p. 012310, Jul 2007. [Online]. Available: <http://link.aps.org/doi/10.1103/PhysRevA.76.012310>
- [26] V. Karimipour and L. Memarzadeh, "Entanglement and optimal strings of qubits for memory channels," *Phys. Rev. A*, vol. 74, p. 062311, Dec 2006. [Online]. Available: <http://link.aps.org/doi/10.1103/PhysRevA.74.062311>
- [27] Z. Shadman, H. Kampermann, D. Bruß, and C. Macchiavello, "Optimal superdense coding over memory channels," *Phys. Rev. A*, vol. 84, p. 042309, Oct 2011. [Online]. Available: <http://link.aps.org/doi/10.1103/PhysRevA.84.042309>
- [28] G. Bowen and S. Mancini, "Quantum channels with a finite memory," *Phys. Rev. A*, vol. 69, p. 012306, Jan 2004. [Online]. Available: <http://link.aps.org/doi/10.1103/PhysRevA.69.012306>
- [29] N. Arshed and A. H. Toor, "Entanglement-assisted classical capacity of quantum channels with correlated noise," *Phys. Rev. A*, vol. 73, p. 014304, Jan 2006. [Online]. Available: <http://link.aps.org/doi/10.1103/PhysRevA.73.014304>
- [30] A. D'Arrigo, G. Benenti, and G. Falci, "Quantum capacity of dephasing channels with memory," *New Journal of Physics*, vol. 9, no. 9, p. 310, 2007. [Online]. Available: <http://stacks.iop.org/1367-2630/9/i=9/a=310>
- [31] A. D'Arrigo, E. D. Leo, G. Benenti, and G. Falci, "Memory effects in a Markov chain dephasing channel," *International Journal of Quantum Information*, vol. 06, no. supp01, pp. 651–657, 2008.
- [32] C. Cafaro and S. Mancini, "Repetition versus noiseless quantum codes for correlated errors," *Physics Letters A*, vol. 374, no. 26, pp. 2688 – 2700, 2010. [Online]. Available: <http://www.sciencedirect.com/science/article/pii/S037596011000486X>
- [33] ———, "Quantum stabilizer codes for correlated and asymmetric depolarizing errors," *Phys. Rev. A*, vol. 82, p. 012306, Jul 2010. [Online]. Available: <http://link.aps.org/doi/10.1103/PhysRevA.82.012306>
- [34] P. Huang, G. He, Y. Lu, and G. Zeng, "Quantum capacity of pauli channels with memory," *Physica Scripta*, vol. 83, no. 1, p. 015005, 2011. [Online]. Available: <http://stacks.iop.org/1402-4896/83/i=1/a=015005>
- [35] C. Cafaro and S. Mancini, "Concatenation of error avoiding with error correcting quantum codes for correlated noise models," *International Journal of Quantum Information*, vol. 09, no. supp01, pp. 309–330, 2011.
- [36] J. P. Clemens, S. Siddiqui, and J. Gea-Banacloche, "Quantum error correction against correlated noise," *Phys. Rev. A*, vol. 69, p. 062313, Jun 2004. [Online]. Available: <http://link.aps.org/doi/10.1103/PhysRevA.69.062313>
- [37] H. V. Nguyen, Z. Babar, D. Alanis, P. Botsinis, D. Chandra, S. X. Ng, and L. Hanzo, "EXIT-chart aided quantum code design improves the normalised throughput of realistic quantum devices," *IEEE Access*, vol. 4, pp. 10194–10209, 2016.
- [38] K. Kraus, "General state changes in quantum theory," *Annals of Physics*, vol. 64, pp. 311–335, Jun. 1971.
- [39] M. A. Nielsen and I. L. Chuang, *Quantum Computation and Quantum Information: 10th Anniversary Edition*, 10th ed. New York, NY, USA: Cambridge University Press, 2011.
- [40] C. Lupo, V. Giovannetti, and S. Mancini, "Memory effects in attenuation and amplification quantum processes," *Phys. Rev. A*, vol. 82, p. 032312, Sep 2010. [Online]. Available: <http://link.aps.org/doi/10.1103/PhysRevA.82.032312>
- [41] V. Giovannetti, "A dynamical model for quantum memory channels," *Journal of Physics A: Mathematical and General*, vol. 38, no. 50, p. 10989, 2005. [Online]. Available: <http://stacks.iop.org/0305-4470/38/i=50/a=008>
- [42] C. H. Bennett and P. W. Shor, "Quantum channel capacities," *Science*, vol. 303, no. 5665, pp. 1784–1787, 2004. [Online]. Available: <http://science.sciencemag.org/content/303/5665/1784>
- [43] R. Jahangir, N. Arshed, and A. H. Toor, "Quantum capacity of an amplitude-damping channel with memory," *Quantum Information Processing*, vol. 14, no. 2, pp. 765–782, Feb. 2015. [Online]. Available: <http://dx.doi.org/10.1007/s11128-014-0883-y>
- [44] C. H. Bennett, D. P. DiVincenzo, J. A. Smolin, and W. K. Wootters, "Mixed-state entanglement and quantum error correction,"

Phys. Rev. A, vol. 54, pp. 3824–3851, Nov 1996. [Online]. Available: <http://link.aps.org/doi/10.1103/PhysRevA.54.3824>

[45] G. Zhu and F. Alajaji, “Joint source-channel turbo coding for binary Markov sources,” IEEE Trans. Wireless Commun., vol. 5, no. 5, pp. 1065–1075, May 2006.

[46] J. Garcia-Frias and J. D. Villasenor, “Combining hidden Markov source models and parallel concatenated codes,” IEEE Commun. Lett., vol. 1, no. 4, pp. 111–113, Jul. 1997.

[47] M. A. M. Izhar, N. Fisal, X. Zhou, K. Anwar, and T. Matsumoto, “Exploitation of 2D binary source correlation using turbo block codes with fine-tuning,” EURASIP J. Wirel. Commun. Netw., vol. 2013, no. 89, pp. 1–11, Mar. 2013.

[48] S. ten Brink, “Convergence behavior of iteratively decoded parallel concatenated codes,” IEEE Trans. Commun., vol. 49, no. 10, pp. 1727–1737, Oct. 2001.

[49] L. Hanzo, T. H. Liew, B. L. Yeap, R. Y. S. Tee, and S. X. Ng, Turbo Coding, Turbo Equalisation and Space-Time Coding: EXIT-Chart-Aided Near-Capacity Designs for Wireless Channels, 2nd Edition. New York, NY, USA: Wiley-IEEE Press, 2011.

[50] A. Grant, “Convergence of non-binary iterative decoding,” in Global Telecommunications Conference, 2001. GLOBECOM ’01. IEEE, vol. 2, 2001, pp. 1058–1062 vol.2.

[51] J. Kliewer, S. X. Ng, and L. Hanzo, “Efficient computation of EXIT functions for nonbinary iterative decoding,” IEEE Trans. Commun., vol. 54, no. 12, pp. 2133–2136, Dec. 2006.

[52] M. Adrat, P. Vary, and J. Spittka, “Iterative source-channel decoder using extrinsic information from softbit-source decoding,” in Proc. of IEEE Int. Conf. Acoustics, Speech and Signal Processing, Utah, USA, May 2001, pp. 2653–2656.

[53] Y. Huo, C. Zhu, and L. Hanzo, “Spatio-temporal iterative source-channel decoding aided video transmission,” IEEE Trans. Veh. Technol., vol. 62, no. 4, pp. 1597–1609, May 2013.



MOHD AZRI MOHD IZHAR received his M.Eng. degree in electrical engineering (communications) from the University of Sheffield, U.K., in 2008 where he received the Mappin medal award for outstanding academic performance and the Institute of Electrical and Electronics Engineers (IEEE) prize for the best communication-related final year project. He received the Ph.D. degree in electrical engineering from the Universiti Teknologi Malaysia (UTM), Malaysia, in 2014. Since 2014, he has been a senior lecturer with the UTM Kuala Lumpur campus. He was visiting the Southampton Wireless Group at the University of Southampton, U.K. for 2 years in 2015. His current research interests include channel coding, coding theory, joint source-channel coding, coded modulation, cooperative communications, cognitive radio and quantum communications.



PANAGIOTIS BOTSINIS (S'12) received the M.Eng. degree from the School of Electrical and Computer Engineering of the National Technical University of Athens (NTUA), Greece, in 2010, as well as the M.Sc. degree with distinction and the Ph.D. degree in Wireless Communications from the University of Southampton, UK, in 2011 and 2015, respectively. He is currently working as a Research Fellow in the Southampton Wireless group at the School of Electronics and Computer Science of the University of Southampton, UK. Since October 2010, he has been a member of the Technical Chamber of Greece. His research interests include quantum-assisted communications, quantum computation, iterative detection, OFDM, MIMO, multiple access systems, coded modulation, channel coding, cooperative communications, as well as combinatorial optimization.



ZUNAIRA BABAR received her B.Eng. degree in electrical engineering from the National University of Science & Technology (NUST), Islamabad, Pakistan, in 2008, and the M.Sc. degree (Distinction) and the Ph.D. degree in wireless communications from the University of Southampton, UK, in 2011 and 2015, respectively. She is currently working as a Research Fellow in the Southampton Wireless group at the University of Southampton. Her research interests include quantum error correction codes, channel coding, coded modulation, iterative detection and cooperative communications.



DIMITRIOS ALANIS (S'13) received the M.Eng. degree in Electrical and Computer Engineering from the Aristotle University of Thessaloniki in 2011 and the M.Sc. degree in Wireless Communications from the University of Southampton in 2012. He is currently working towards the PhD degree with the Southampton Wireless (SW) Group, School of Electronics and Computer Science of the University of Southampton. His research interests include quantum computation and quantum information theory, quantum search algorithms, cooperative communications, resource allocation for self-organizing networks, bio-inspired optimization algorithms and classical and quantum game theory.



HUNG VIET NGUYEN received the B.Eng. degree in electronics and telecommunications from the Hanoi University of Science and Technology, Hanoi, Vietnam, in 1999, the M.Eng. degree in telecommunications from the Asian Institute of Technology, Bangkok, Thailand, in 2002, and the Ph.D. degree in wireless communications from the University of Southampton, Southampton, U.K., in 2013. Since 1999, he has been a Lecturer with the Posts and Telecommunications Institute of Technology, Vietnam. He is involved in the OPTIMIX and CONCERTO European as well as EPSRC funded projects. He is currently a Research Fellow with the 5G Innovation Centre, University of Surrey, U.K. His research interests include cooperative communications, channel coding, network coding, and quantum communications.



DARYUS CHANDRA received the M.Eng. degree in electrical engineering from Universitas Gadjah Mada (UGM), Indonesia, in 2014. He is currently pursuing the Ph.D. degree with the Southampton Wireless group, School of Electronics and Computer Science, University of Southampton. He is a recipient of scholarship award from Indonesia Endowment Fund for Education (LPDP). His research interests include channel codes, quantum error correction codes, and quantum communications.



**DR SOON XIN NG** (S'99-M'03-SM'08) received the B.Eng. degree (First class) in electronic engineering and the Ph.D. degree in telecommunications from the University of Southampton, Southampton, U.K., in 1999 and 2002, respectively. From 2003 to 2006, he was a postdoctoral research fellow working on collaborative European research projects known as SCOUT, NEWCOM and PHOENIX. Since August 2006, he has been a member of academic staff in the School of Electronics and Computer Science, University of Southampton. He is involved in the OPTIMIX and CONCERTO European projects as well as the IU-ATC and UC4G projects. He is currently an Associate Professor in telecommunications at the University of Southampton.

His research interests include adaptive coded modulation, coded modulation, channel coding, space-time coding, joint source and channel coding, iterative detection, OFDM, MIMO, cooperative communications, distributed coding, quantum error correction codes and joint wireless-and-optical-fibre communications. He has published over 200 papers and co-authored two John Wiley/IEEE Press books in this field. He is a Senior Member of the IEEE, a Chartered Engineer and a Fellow of the Higher Education Academy in the UK.



**LAJOS HANZO** (<http://www-mobile.ecs.soton.ac.uk>) FREng, FIEEE, FIET, Fellow of EURASIP, DSc received his 5-year Master degree in electronics in 1976, and the Doctoral degree in 1983. In 2009 he was awarded an honorary doctorate by the Technical University of Budapest and in 2015 by the University of Edinburgh. In 2016 he was admitted to the Hungarian Academy of Science. During his 40-year career in telecommunications he has held various research and academic posts in Hungary, Germany and the UK. Since 1986 he has been with the School of Electronics and Computer Science, University of Southampton, UK, where he holds the chair in telecommunications. He has successfully supervised 111 PhD students, co-authored 18 John Wiley/IEEE Press books on mobile radio communications totalling in excess of 10 000 pages, published 1701 research contributions at IEEE Xplore, acted both as TPC and General Chair of IEEE conferences, presented keynote lectures and has been awarded a number of distinctions. Currently he is directing a 60-strong academic research team, working on a range of research projects in the field of wireless multimedia communications sponsored by industry, the Engineering and Physical Sciences Research Council (EPSRC) UK, the European Research Council's Advanced Fellow Grant and the Royal Society's Wolfson Research Merit Award.

He is an enthusiastic supporter of industrial and academic liaison and he offers a range of industrial courses. He is also a Governor of the IEEE VTS and ComSoc. During 2008 - 2012 he was the Editor-in-Chief of the IEEE Press and a Chaired Professor also at Tsinghua University, Beijing. For further information on research in progress and associated publications please refer to <http://www-mobile.ecs.soton.ac.uk> Lajos has 33 000+ citations and an H-index of 73.

• • •